

# HEUSLER THERMOELECTRIC ALLOY OBTAINED BY SOLID STATE REACTION

V. CEBOTARI<sup>1</sup>      N.A. SECHEL<sup>1</sup>  
P. PAŞCUŢA<sup>2</sup>      F. POPA<sup>1</sup>

**Abstract:** *The thermoelectric alloy  $Ni_{51}Mn_{19}Sn_{30}$  was obtained by mechano-synthesis, from elemental powders in a planetary ball mill. The milling was carried out in the argon atmosphere for 4 h and 10 h. The structural evolution was studied by X-ray diffraction. At 4 h a mixture of phases was found. After 10 h of milling, a complete reaction leads to the formation of the Heusler  $Ni_2MnSn$  alloy was observed. The morphological characterisation of the powder has been performed using scanning electron microscopy (SEM). The particle shape changes upon milling, leading to irregular shaped particles of small dimension. The particle size distribution indicates that milling leads to fragmentation of powders.*

**Key words:** *heusler alloy, mechanical alloying, nanocrystalline, thermoelectric.*

## 1. Introduction

Energy conversion represents a relative novel field of research, aiming the minimisation of environmental pollution as much as possible [2]. One of the studied research directions is refrigeration, namely magnetic refrigeration. Heusler alloys are of major importance in this context, because they have a low Curie temperature, close to room temperature, and this feature makes them applicable to energy conversion. This can be accomplished by using the transition from ferromagnetic to paramagnetic state, which occurs with a heat release; with this transition, you can heat or cool an enclosure.

Heusler alloys are named after German engineer Friedrich Heusler mining and chemist who discovered ferromagnetism in Mn-Al alloy, where the constituting elements are all non-ferromagnetic, but the compound is ferromagnetic [1]. Heusler alloys are ternary intermetallic compounds with a stoichiometric  $X_2YZ$ , known as the "full-Heusler" and with the stoichiometry of  $XZY$ , known as the "half-Heusler" [1], [7]. The full-Heusler alloys crystallize in the  $L2_1$  structure, where X can be one of the elements Fe, Co, Ni etc. Y may be a transition element, and Z may be an element from groups III, IV or V [12]. Generally, the Heusler structure can be described as consisting of four interpenetrating face centered cubic lattices where the X atoms occupy the A (0,0,0) and C (1/2, 1/2, 1/2) sites. The Y atom occupies the B (1/4, 1/4, 1/4) sites and the Z atom occupies the D (3/4, 3/4, 3/4) sites. It has been noticed that the preferred positions of the X and Y atoms are strongly influenced by the number of electrons on the 3d layer. The elements with the

---

<sup>1</sup> Materials Science and Engineering Dept., Technical University of Cluj-Napoca, Romania.

<sup>2</sup> Physics and Chemistry Dept., Technical University of Cluj-Napoca, Romania.

higher 3d electrons occupy preferentially the A, C sites, whereas the elements with lower number of 3d electrons tends to occupy the B site [1]. When the Y atom is Mn, the Heusler alloys are magnetic. Complex studies on the structural and magnetic properties of the  $\text{Ni}_2\text{Mn}_{1-x}\text{Z}_x$  alloys were carried out by T. Krenke [1]. Many of these alloys possess super magnetic elasticity and magnetocaloric effect [1], [12].

The classical way for obtaining the Heusler alloys is by arc-melting of the elements. For the arc-melted Ni-Mn-Sn alloys was proved the importance of heat treatment at high temperature to ensure the homogeneity of the structure. It must be mentioned, that the heat treatments were performed at high temperatures and large time durations [5], [8].

The Ni-Mn-Sn system manifests a crystallographic transition, from  $L2_1$  structure to a layered martensitic structure [10], [11]. The thermoelectric properties were found to be depended on the density of states at Fermi level. The density of states modify with crystallographic changes and at transition a sharp variation was recorded [4]. The magnetic properties differs in the two states, the martensitic phase presents lower magnetization. Martensitic phase also shows the electrical resistance of two times greater as compared with the austenitic phase [10], [11].

In order to introduce the nanocrystalline state into the Heusler alloy, the mechanical alloying was used. Mechanical alloying represents a process for the production of alloys by solid stated reaction. The process consists in repetitive fragmentation and cold welding events of initial powders, leading to mixing, homogenization and finally alloying. By mechanical alloying new materials are obtained, some of which are impossible to achieve with conventional methods. The materials that are obtained by mechanical alloying are: nanomaterials, solid solutions, supersaturated solid solutions and amorphous materials [3], [9].

The present paper studies the obtaining of the  $\text{Ni}_{51}\text{Mn}_{19}\text{Sn}_{30}$  non-stoichiometric alloy by mechanical alloying and the influence of the alloying process on the structure, morphology and particle size of the powder.

## 2. Experimental

To obtain the  $\text{Ni}_{51}\text{Mn}_{19}\text{Sn}_{30}$  alloy by mechanosynthesis, a mixture of Ni, Mn and Sn elemental powders was used. Before milling, the powders were homogenised for 15 minutes using a Turbula type spatial homogenizer. Mechanical alloying of the powders was performed using the planetary ball mill type Fritsch Pulverisette 4. The powder was placed into a stainless steel container, with a volume of  $250 \text{ cm}^3$  together with stainless steel balls with a diameter of 14 mm. The used milling atmosphere was high purity argon. The filling factor of the container was 35% and the weight ball to powder ratio (BPR) 8:1. Sampling was done at different milling intervals: 0, 4 and 10 hours. At each of these milling intervals, the mass of the samples was around 5 g. The structural characterization of the alloy was studied by X-ray diffraction (XRD) with a Shimadzu XRD-6000 diffractometer operating with  $\text{Co K}\alpha$  ( $\lambda = 1.54183 \text{ \AA}$ ) radiation in the angular range  $2\theta$  20-100°. The particle size distribution of the powders resulting from the mechanosynthesis process was recorded using an Analysette 22 Nano Tec particle analyser. The size range was from 0.1  $\mu\text{m}$  to 135  $\mu\text{m}$ . From the particle size distribution, the parameters D10, D50 and D90 were determinate. D10, D 50 and D90 represents the mean powder diameter equal with a diameter more or equal with 10, 50 and 90 % from the total powder volume [6]. In order to study the morphology of the obtained powder,

the JEOL-JSM 5600 LV scanning electronic microscope (SEM), equipped with an Energy dispersive X-ray microanalysis EDX spectrometer (Oxford Instruments - INCA 200 software) was used.

### 3. Results and Discussion

The X-ray diffraction patterns (XRD) corresponding to the starting elemental mixture, noted with 0 h, and for the  $\text{Ni}_{51}\text{Mn}_{19}\text{Sn}_{30}$  alloy, milled for 4 and 10 hours are presented in Figure 1. After 4 hours of milling, the characteristic peaks corresponding to manganese and tin are no longer visible, while the nickel characteristic peaks are fading. This suggests that the solid state reaction of the elemental powders has occurred. Leading to the formation  $\text{Ni}_{51}\text{Mn}_{19}\text{Sn}_{30}$  alloy as can be seen in the XRD pattern corresponding to the sample milled for 4 hours. After 4 hours of milling, in the material, two new phases, identified as belonging to the full Heusler and respectively Half Heusler are found. Further milling up to 10 hours leads to the disappearance of the diffraction peak corresponding to the elemental powders. At this point, only the reacted Ni-Mn-Sn phases are observed in the material.

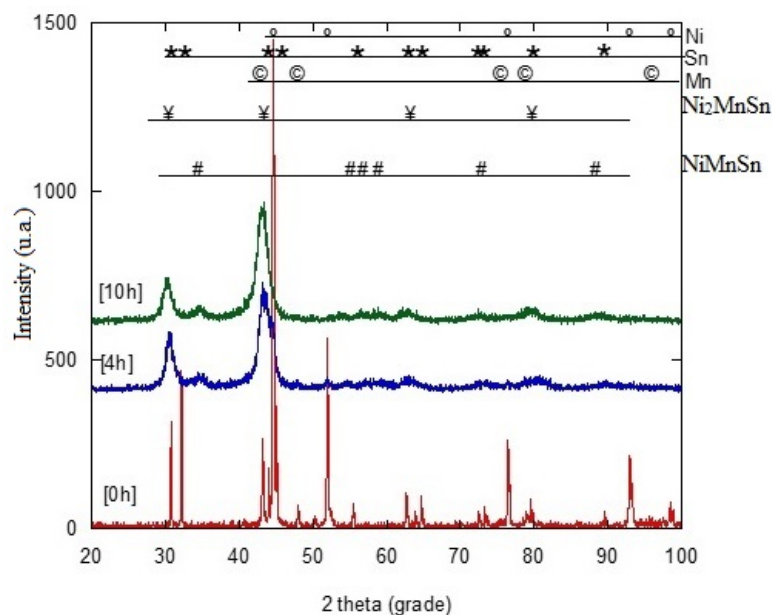


Fig. 1. XRD patterns corresponding to the samples milled for 0 h, 4 h and 10 h, for  $\text{Ni}_{51}\text{Mn}_{19}\text{Sn}_{30}$

Another aspect worth to mention is the peak broadening upon increasing milling duration. This occurs due to internal stresses induced in the material by the mechanical milling. Besides this, the crystallite size reduction also leads to broader peaks, as compared to the starting sample. Upon increasing milling duration up to 10 hours, no new phases are observed in the material. The XRD peaks are experiencing only broadening, due to crystallite size reduction.

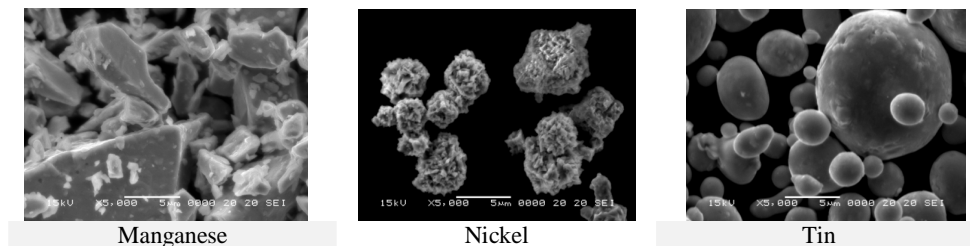


Fig. 2. The particle image of Mn, Ni and Sn used for the initial mixture

The morphological characterization of the mechanically alloyed samples was performed by scanning electron microscopy (SEM). For comparison, SEM images were recorded also for the starting powders. The images obtained on the elemental powders of Mn, Ni and Sn are shown in Figure 2. The Mn powder falls into the category of sharp powder types, the elemental Ni powder has a spongy aspect. And the tin powder has the spherical shape characteristic of the liquid atomization process.

The study of the morphology of the  $\text{Ni}_{51}\text{Mn}_{19}\text{Sn}_{30}$  powder versus milling duration is shown in Figure 3a. Figure 3a, shows a trend that depends on the milling time. The starting sample shows the mixture of elemental powders, clearly observing the three types of powders used. The image corresponding to the mechanically alloyed powder for 4 hours shows a total change compared to the image of the starting sample. In this image, we have a single type of particles that are made up of small particle agglomerates that are the result of altering the elementary powders. Between 4 and 10 hours of milling the particle size increases, and their appearance becomes irregular. Also, the larger particles are in fact, agglomerations of smaller particles welded together after 4 hours milling.

The particle size distribution of the  $\text{Ni}_{51}\text{Mn}_{19}\text{Sn}_{30}$  alloy is shown in Figure 3b. For the starting sample, it is found that the homogenised powder shows a Gaussian type distribution and the peak of the curve is around  $10\ \mu\text{m}$ . Gaussian distribution is the result of very good homogenization of elemental powder particles; the three particle types have similar particle sizes.

The particle size distribution of the 4 hours milled samples reveals a slight assymetry, due to the presence of another peak. These two peaks may exist due to the presence of the two phases -  $\text{Ni}_{51}\text{Mn}_{19}\text{Sn}_{30}$  alloys and unreacted nickel. The granulometric distribution for the milled sample for 10 hours has a single broad maximum. This flattening is the effect complete reaction of elemental powders.

The average particle size for the  $\text{Ni}_{51}\text{Mn}_{19}\text{Sn}_{30}$  composition was outlined using the distributions of Figure 3b, as shown in Figure 4. In the case of D10 the particle size decreases slightly up to 4 hours of milling. Increasing milling time from up to 10 hours of milling has no significant effect on the particle size, which remains approximately constant. The decrease of D10 for milled samples is the effect of fragmentation of powders, particularly the tough component. In the case of D50 parameter, the powder particle size decreases slightly upon milling. This can be explained by the fact that the phases that are formed keep the same size as the original particles. Throughout the milling process, fragmentation and cold welding processes remain in balance. In the case of D90, the particle diameter increases for 0 to 4 hours of milling due to the cold welding process. Probably these large particles represent the  $\text{Ni}_{51}\text{Mn}_{19}\text{Sn}_{30}$  alloy particles that are formed during milling. This is also observed in the images obtained by SEM, where for

the sample milled for 4 hours, larger particles on which smaller particles are welded have been observed. After obtaining a sufficiently large amount of the thermoelectric alloy, the D90 slightly due to the homogenization of the composition and the stabilisation of the ratio between fragmentation and cold weld induced milling.

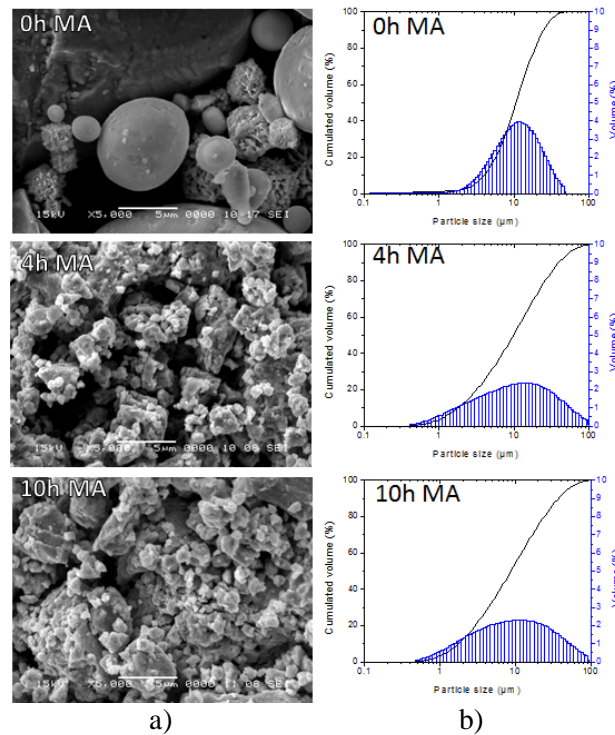


Fig. 3. Scanning electron microscope images recorded for  $Ni_{51}Mn_{19}Sn_{30}$  alloy milled 0, 4 and 10 h (a). Particle size distribution of the powder corresponding to the milling times presented in the SEM images (b)

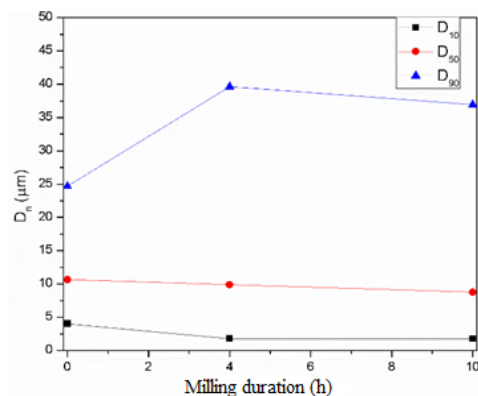


Fig. 4. D10, D50 and D90 evolution with milling time

Concerning the crystallite size, estimated from the broadening of the diffraction peaks, can be estimate to be in the nanometric range.

#### 4. Conclusion

The mechano-synthesis of the  $\text{Ni}_{51}\text{Mn}_{19}\text{Sn}_{30}$  alloy is complex. After 10 hours of milling, the alloy consists of a biphasic mixture ( $\text{Ni}_2\text{MnSn}$  and  $\text{NiMnSn}$ ). Heusler phases are present in samples after 4 hours of milling. The morphology of elemental powders changes significantly due to milling, and the alloy is formed of small, agglomerated particles. The particle size distribution indicates that the  $\text{Ni}_{51}\text{Mn}_{19}\text{Sn}_{30}$  phase forms larger particles.

#### References

1. Aksoy, S.: *Magnetic Interactions in Martensitic Ni-Mn Based Heusler Systems*. In: Fakultät für Physik der Universität Duisburg-Essen. [www.uni-due.de/agfarle/PDF/dipl-doc/DissAksoy.pdf](http://www.uni-due.de/agfarle/PDF/dipl-doc/DissAksoy.pdf). Accessed: 28.04.2017.
2. Bashir, M.B.A., Said, S.M., Sabri, M.F.M., Shnawah, D.A., Elsheikh, M.H.: *Recent Advances on  $\text{Mg}_2\text{Si}_{1-x}\text{Sn}_x$  Materials for Thermoelectric Generation*. In: *Renewable and Sustainable Energy Reviews* **37** (2014), p. 569-584.
3. Gaffet, E., Le Caër, G.: *Mechanical Processing for Nanomaterials*. In: *Encyclopedia of Nanoscience and Nanotechnology* (2004), p. 1-39.
4. Koyama, K., Igarashi, T., Okada, H., Watanabe, K., Kanomata, T., Kainuma, R., Ito, W., Oikawa, K., Ishida, K.: *Magnetic and Thermoelectric Properties of  $\text{Ni}_{50}\text{Mn}_{36}\text{Sn}_{14}$  in High-Magnetic Fields*. In: *Journal of Magnetism and Magnetic Materials* **310** (2007), p. e994-e995.
5. Liu, F.S., Wang, Q.B., Li, S.P., Ao, W.Q., Li, J.Q.: *The Martensitic Transition and Magnetocaloric Properties of  $\text{Ni}_{51}\text{Mn}_{49-x}\text{Sn}_x$* . In: *Physica B* **412** (2013), p. 74-78.
6. Marinca, T.F., Chicinaş, H.F., Neamţu, B.V., Chicinaş, I., Isnard, O., Popa, F., Păscuţă, P.: *Nanocrystalline/nanosized  $\text{Fe}_3\text{O}_4$  Obtained by a Combined Route Ceramic-Mechanical Milling. Effect of Milling on the Chemical Composition, Formation of Phases and Powder Characteristics*. In: *Advanced Powder Technology* **27** (2016), p. 1588-1596.
7. Podgornykh, S.M., Streltsov, S.V., Kazantsev, V.A., Shreder, E.I.: *Heat Capacity of Heusler Alloys: Ferromagnetic  $\text{Ni}_2\text{MnSb}$ ,  $\text{Ni}_2\text{MnSn}$ ,  $\text{NiMnSb}$  and Antiferromagnetic  $\text{CuMnSb}$* . In: *Journal of Magnetism and Magnetic Materials* **311** (2007), p. 530-534.
8. Ray, M.K., Bagani, K., Banerjee, S.: *Effect of Excess Ni on Martensitic Transition, Exchange Bias and Inverse Magnetocaloric Effect in  $\text{Ni}_{2+x}\text{Mn}_{1.4-x}\text{Sn}_{0.6}$  Alloy*. In: *Journal of Alloys and Compounds* **600** (2014), p. 55-59.
9. Suryanarayana, C.: *Mechanical Alloying and Milling*. In: *Progress in Materials Science* **46** (2001), p. 1-184.
10. Wang, S., Cheng, H., Wu, R., Chao, W.: *Structural and Thermoelectric Properties of  $\text{HfNiSn}$  Half-Heusler Thin Films*. In: *Thin Solid Films* **518** (2010), p. 5901-5904.
11. Ye, M., Kimura, A., Miura, Y., Shirai, M.Y., Cui, T., Shimada, K., Namatame, H., Taniguchi, M., Ueda, S., Kobayashi, K., Kainuma, R., Shishido, T., Fukushima, K., Kanomata, T.: *Role of Electronic Structure in the Martensitic Phase Transition of  $\text{Ni}_2\text{Mn}_{1+x}\text{Sn}_{1-x}$  Studied by Hard-X-Ray Photoelectron Spectroscopy and Ab Initio Calculation*. In: *Physic Review Letters* **104** (2010), 176401.
12. Zenasni, H., Faraoun, H.I., Esling, C.: *First-Principle Prediction of Half-Metallic Ferrimagnetism in Mn-Based Full-Heusler Alloys with Highly Ordered Structure*. In: *Journal of Magnetism and Magnetic Materials* **333** (2013), p. 162-168.